Impact of land-use on PAH transfer in sub-surface water as recorded by CaCO3 concretions in urban underground structures (Paris, France).

Julia Garagnon, Emmanuel Naffrechoux, Yves Perrette, Emmanuel Dumont, Phillipe Branchu, Jules Querleux, Gael Monvoisin, Mathieu Pin, Delphine Tisserand, Edwige Pons-Branchu

Environmental Pollution 357 (2024) 124437

Contents lists available at ScienceDirect

Environmental Pollution

journal homepage: www.elsevier.com/locate/envpol

Impact of land-use on PAH transfer in sub-surface water as recorded by $CaCO_3$ concretions in urban underground structures (Paris, France)☆

Julia Garagnon [a,b,*], Emmanuel Naffrechoux [b], Yves Perrette [b], Emmanuel Dumont [c], Phillipe Branchu [c], Jules Querleux [d], Gael Monvoisin [e], Mathieu Pin [b], Delphine Tisserand [f], Edwige Pons-Branchu [a]

[a] LSCE/IPSL, UMR 8212 (CEA-CNRS-UVSQ), Université Paris-Saclay, Orme des Merisiers F-91191 Gif-sur-Yvette, France
[b] EDYTEM (CNRS/USMB), Bâtiment Pole Montagne, Campus Scientifique, 73376 Le Bourget du Lac Cedex, France
[c] CEREMA: TEAM - 12 Rue Teisserenc de Bort, 78197 TRAPPES-en-Yvelines Cedex; and 58 rue Roger Salengro - Boîte 121 Immeuble Dolomites - Bât. D / 94120 Fontenay-sous-Bois France
[d] IGC, Inspection générale des Carrières, 86 rue Regnault, 75013, France
[e] Laboratoire GEOPS, Université. Paris Saclay, UMR 8148 CNRS – Université Paris Saclay, 91405, Orsay Cedex, France
[f] ISTerre, Univ. Grenoble Alpes, Univ. Savoie Mont Blanc, CNRS, IRD, Univ. Gustave Eiffel, F-38000, Grenoble, France

ARTICLE INFO

Keywords:
Water quality
PAHs
Organic pollution
Urbanization
Speleothem
Soil

ABSTRACT

In densely populated urban areas, the pressure on water resources is considerable and will tend to intensify over the next decades. Preserving water resources therefore seems fundamental, but many questions remain as to the transfer of contaminants to subsurface waters in these largely sealed areas. Because of their toxicity and persistence in the environment, this work focused on the study of polycyclic aromatic hydrocarbons (PAHs), ubiquitous pollutants mainly produced by human activities. To better understand the main factors leading to the retention or transport of these pollutants in urban environments, vertical transects, from the surface to several meters down, were established on three study sites in or near Paris (France), selected according to an urbanization gradient. Soil samples collected at the surface and urban secondary carbonate deposits (USCD), similar to cave speleothems, sampled underground in quarries and aqueducts were analyzed. As the hydrophobic properties of PAHs favor their sorption onto organic matter, the latter was also studied using organic carbon analysis and UV fluorescence spectroscopy. The USCD located closest to the urbanized surface contained high concentrations of PAHs (76.8 ± 5.3 ng g^{-1}), while the USCD located at greater depth with organic soil on the surface contained the lowest amount of PAHs (2.9 ± 0.4 ng g^{-1}), and no PAHs with log $K_{OC} > 5$. The results highlight the predominant role played by the presence of organic topsoil at the surface in retaining and storing large amounts of PAHs (1914–2595 ng. g_{soil}^{-1}), particularly the most hydrophobic ones (i.e. 60% of the 15 PAHs are characterized by a Log $K_{OC} > 5$), which are also the most toxic. The lithology and thickness of the bedrock (between the surface and the USCD) also play an important role in the retention of PAHs, particularly those adsorbed on the particulate phase.

1. Introduction

Today, around half of the world's population lives in urban areas, a proportion that is expected to exceed 68 % by 2050 (United Nations-Population Division, 2019). In these densely populated areas, the pressure on water resources is significant and is likely to intensify in the coming years as a result of climate change (Flörke et al., 2018; Ligtvoet et al., 2014). Turning to alternative resources by using non-conventional water sources such as spring water or subsurface water for specific purposes (e.g. irrigating green spaces or cleaning streets) could help to reduce drinking water consumption and overcome water scarcity in these areas. However, groundwater is threatened by pollution carried from the surface by rainwater infiltration (e.g. agricultural chemicals, organic or chemical pollutant emissions from residential or industrial

☆ This paper has been recommended for acceptance by Prof. Dr. Klaus Kümmerer.

* Corresponding author. LSCE/IPSL, UMR 8212 (CEA-CNRS-UVSQ), Université Paris-Saclay, Orme des Merisiers F-91191 Gif-sur-Yvette, France.
E-mail address: julia.garagnon@lsce.ipsl.fr (J. Garagnon).

https://doi.org/10.1016/j.envpol.2024.124437
Received 16 March 2024; Received in revised form 21 June 2024; Accepted 23 June 2024
Available online 24 June 2024

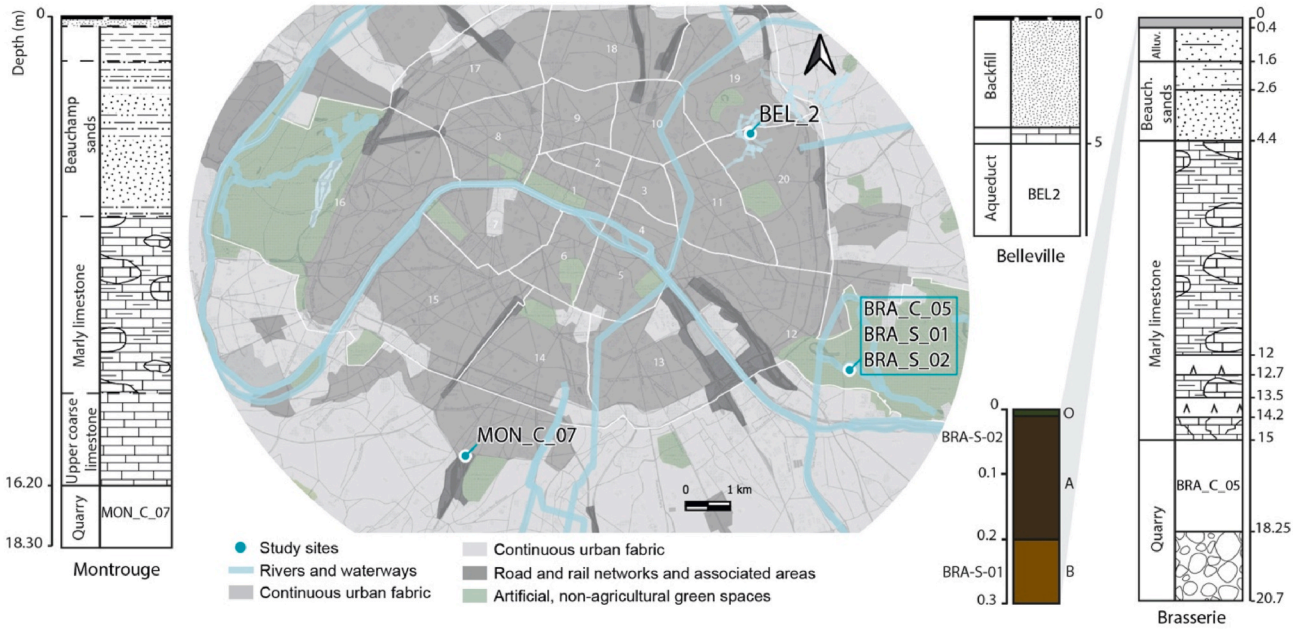

Fig. 1. Simplified land cover map of the Paris region (source: Corine Land Cover Ile de France) and location of each sample. Samples are also located in depth using the log stratigraphy for each site and the cross section of the soil pit at the Brasserie site. Depth is given in meters, lithology is described in the left column of the log stratigraphy and shown schematically in the right column (adapted from USGS codes). For the soil pit, O (for organic), A and B correspond to the different horizons, and colors are taken from the Munsell code. (For interpretation of the references to color in this figure legend, the reader is referred to the Web version of this article.)

areas, atmospheric deposition), and groundwater in urban areas is even more threatened (Burri et al., 2019). The question of the water quality of these potential alternative resources thus remains central, especially as many questions remain about the behavior and prediction of groundwater contaminants. This issue is all the more relevant in urban environments, as it raises questions about the role of soil cover - organic soils vs. Technosols - in contaminant transfer.

Polycyclic aromatic hydrocarbons (PAH) are semi-volatile organic compounds. Sixteen of them are identified as priority pollutants by the US Environmental Protection Agency (US EPA) and the World Health Organization (WHO). PAHs originate both from oil and petroleum products and from the incomplete combustion of organic matter (wood, fossil fuels) (Brown and Peake, 2006; Takada et al., 1991). While the former are leaked or spilled directly onto the soil, the latter are emitted to the atmosphere before returning to the continental surface via dry and wet deposition. Once deposited or accumulated on sealed surfaces, runoff is one of the main pathways for the release of PAHs into the aquatic environment (Müller et al., 2020). Depending on their different physicochemical properties, these pollutants will undergo degradation (photochemical reaction, biodegradation) and/or partitioning (volatilization, sorption, leaching) during transport (Wild and Jones, 1995). Due to their hydrophobic properties, PAHs are particularly prone to bind to dissolved and particulate organic matter (OM) (Jones et al., 1989; Santschi et al., 1997). Thus, PAHs can circulate in sub-surface water in both dissolved form (i.e. solvated directly in water as freely-dissolved PAHs and complexed with dissolved OM) and particulate form, mostly on colloids (Lan et al., 2018; Schwarz et al., 2011). The K_{OC} is the partition coefficient between PAHs dissolved and adsorbed onto particulate organic carbon (i.e. it provides information on the PAH sorption potential onto particulate OM). Today, these persistent organic pollutants are ubiquitous, especially in urban environments (Brown et al., 1996; Coleman et al., 1997; Nielsen et al., 1996; Pereira et al., 1999; Simcik et al., 1997) and their emissions are mainly attributed to anthropogenic activities (Du and Jing, 2018). Their origin and/or temporal evolution has led to numerous studies in natural archives such as marine, lake and river sediments (e.g. Arias et al., 2010; Ayrault et al., 2021; Guo et al., 2007; Pereira et al., 1999). However, PAHs have been very poorly studied in secondary carbonate deposits (speleothems from caves) because of their very low content in these archives and the question of the role of soil and epikarst in their fractionation (Perrette et al., 2008). Similar to cave speleothems, urban secondary carbonate deposits (USCDs) are calcareous deposits formed by dripping or circulating water in artificial urban structures such as aqueducts or quarries. Recent historical studies of these deposits, focusing in particular on the content of OM and PAHs (Garagnon et al., 2023) and Pb, S, REE (Pons-Branchu et al., 2017, 2015; 2014), have demonstrated their potential as recorders of past water quality influenced by human practices and land use.

The main objective of this work was to determine PAH and OM content in quantity and quality in the sub-actual part of USCDs from three contrasting locations in Paris (France) in terms of depths and/or land-use in order to assess the influence of human practices on their transport and accumulation in the USCDs. This multi-site approach was also coupled with complementary analyses of PAHs and OM in soils, and calculations of theoretical predictions of PAHs in seepage water. The aim is to understand the main factors leading to the retention or transport of these pollutants from the surface to sub surface waters, and thus to question the preservation of this water resource.

2. Materials and methods

2.1. Sites and samples

Three sites with different types of urbanization were selected for this study. They are all located in or near Paris (Fig. 1).

- The Belleville site (BEL), located in the northeast of Paris, in the 20th arrondissement, is characterized by a continuous urban fabric. The site is home to the Great Aqueduct of Belleville. This 1050 m long gallery is part of a historic network known as the Northern Springs, which supplied some of the public fountains of Paris between the 12th and 19th centuries (Clément and Thomas, 2016). An urban secondary carbonate deposit, BEL2, was sampled in the central part of the aqueduct. The 45 mm thick sample shows a fine lamination

which, coupled with U–Th analyses, made it possible to estimate that 300 ± 15 years of record are contained in these deposits (Pons--Branchu et al., 2014). The USCD was fed by seepage from the roof of the gallery. The gallery lies at a depth of about 5–10 m below Rue Levert and is covered by a thin layer of Brie limestone and a Technosol (IUSS Working Group WRB, 2022) corresponding to gypsiferous backfill (1–5 m) that is partially sealed.

- The Brasserie site (BRA), located in the southeast of Paris, in the 12th arrondissement, is characterized by a large green space better known as the Bois de Vincennes (995 ha including about 50 % of forest) and considered here as a non-urbanized area. The site under study is a building stone quarry known as the "Brasserie" quarry. It is located at a depth of between 15 and 20 m and covers an area of approximately 4 ha. The Brasserie quarry was excavated between 1741 and 1860 CE in coarse limestone of the middle Lutetian age. It is covered by about 10 m of Upper Lutetian marls and limestones and a remnant of Beauchamp sands (BSS from https://infoterre.brgm.fr/; Inspection Générale des Carrières, 2007) (Fig. 1). BRA-C-05 was collected from a collapse in an area of the quarry where water infiltration is particularly high. Since the upper part of the sample was supplied with water at the time of collection, it is dated to 2019 CE. Using a lamina counting method (Genty and Quinif, 1996) based on a thin section observed under a microscope, the age of the sample was estimated at 76 ± 5 years with an average growth rate of 0.19 mm. yr^{-1}. This age is consistent with the fact that BRA-C-05 grew on a collapse that occurred after the quarry ceased to be active in the year 1860 CE. On the surface, the area is forested. A layer of organic soil of varying thickness (about 0.5 m) overlies alluvial deposits of red/orange sand. Therefore, a soil pit was excavated above the BRA-C-05 sample area. Two soil samples rich in silica (>90 %, Table S1), a typical brown sandy Alocrisol (AFES, 2008; or Hyperdystric Cambisols, FAO, 2006), were taken from this pit (Fig. 1): BRA-S-02 between 0 and 10 cm depth (horizons O/A) and BRA-S-01 between 20 and 30 cm depth (horizon B/Sal). All soil samples were collected from bottom to top in glass jars that had been previously calcined (525°c, 2 h).
- The Montrouge (MON) site, southwest of Paris (Fig. 1), is an industrial railroad site adjacent to residential areas. The Châtillon-Montrouge quarries consist of a vast network of galleries covering three municipalities: Montrouge, Châtillon and Bagneux. Between the 18th and the end of the 19th century (latest date on the quarry face: 1877), they were mainly used to extract coarse-grained limestone for building stone. The galleries are on two, sometimes three, superimposed levels, depending on the benches sought for mining, and are low (between 1 and 2 m). MON-C-07 is a USCD taken in 2019 from a large flowstone still supplied with water, in a gallery on the middle level of the quarry, between 16 m and 18 m deep. As in the Brasserie quarry, the gallery was excavated in coarse Lutetian limestones and is overlain by Upper Lutetian marls and limestones and a layer of Beauchamp sands (BSS from https://infoterre.brgm.fr/; Inspection Générale des Carrières, 2007). The latter is covered by a thin layer of mainly backfill material, which may be similar to a Technosol (IUSS Working Group WRB, 2022) (Fig. 1). From microscopic counting of lamina on a thin section (Genty and Quinif, 1996) it was estimated that 145 years ± 10 years have been recorded in this deposit, i.e. the beginning of the growth in 1874 CE, which seems to correspond to the end of the quarrying.

Only the sub-actual part of the USCDs, corresponding to the top of the samples, was considered in this study. The USCD samples integrate a period of around 15–20 years, between 1995 and 2012 CE for BEL2, 2006 and 2019 CE for BRA-C-05 and 2004 and 2019 CE ± 5 years for MON-C-07.

In addition, the Brasserie site is the only one where organic soil samples could be collected, as the other two study sites are located in urbanized or industrialized areas.

2.2. Analytical

USCDs were sampled for PAH analysis using a wire saw (B.E.A PV cropper/Escil wires) equipped with a 0.6 mm diamond wire and a microdisk to obtain 1 g calcite cubes. Fresh soils were frozen, lyophilized (1–2 mbar, - 58°c) to limit losses or contamination by ambient air, and then sieved to 2 mm. Only the fine fraction of the soil (<2 mm) was analyzed.

2.2.1. PAH extraction and quantification

2.2.1.1. PAH extraction in carbonates. Analyses were performed according to the procedure developed and described by Garagnon et al. (2023). After surface decontamination with dichloromethane (Honeywell, Chromasolv for HPLC) and an ultrasonic bath (3 min, 20 °C, 50–60 kHz, 1000 W), calcite cubes were spiked with 15 ng acenaphtene-d10, anthracene-d10, and benzo[a]anthracene-d-12 (AccuStandard Certified Reference Materials) to calculate PAH uncertainties.

Calcite was then dissolved by manual agitation with the addition of 10 mL HCL (Carlo Elba, 34–37% RS Superpure for trace analysis) in 15 mL dichloromethane and 5 mL UHQ water (Maxima USF Elga, 18.2 MΩ). Five milliliters of solvent were extracted from the emulsion in a separate tube. Two successive liquid/liquid extractions were then performed with 5 mL of dichloromethane each. Sodium sulfate powder was added to the 15 mL extract to remove residual water, then concentrated at 40 °C under nitrogen flow in an automated evaporator (TurboVap II, Caliper Life Sciences) to a volume of 1 mL. After filtration at 0.22 μm (PTFE filters), 100 μL dimethyl sulfoxide (DMSO, Thermo Scientific, LC-MS grade) was added and evaporation was continued gently under reduced nitrogen pressure to a final volume of 100 μL. Samples were then taken up with 100 μL of methanol and kept cool prior to analysis. Blanks were also produced using the same protocol steps.

2.2.1.2. PAH extraction in soils. The protocol is based on that described by Marchal et al. (2023). Soil samples and blanks were spiked with 250 μL of a solution containing 100 ng mL^{-1} of acenaphtene-d10, anthracene-d10 and benzo[a]anthracene-d12. Three liquid/liquid extractions were performed on 5 g of soil using 15 mL of dichloromethane/acetone mixture (80:20), an ultrasonic bath (3 min, 50–60 kHz, 1000 W) and centrifugation for 10 min at 1600 rpm to separate the solid phase from the solvent. The 45 mL of solvent was then concentrated to 1 mL under nitrogen flow in a Turbovap by rinsing the tube walls with heptane after 20 min. Sodium sulfate powder was added to remove residual water and the samples were then filtered at 0.22 μm using PTFE filters. To prevent volatilization of PAHs, 100 μL DMSO was added and evaporation was continued gently under reduced nitrogen pressure to a final volume of 100 μL. The samples were then taken up with 1000 μL of methanol, filtered again at 0.22 μm and kept cool before analysis.

2.2.1.3. PAH quantification. A total of 15 PAHs among de 16 PAHs of the US-EPA list were analyzed: naphthalene (N), acenaphthene (ACE), fluorene (FLU), phenanthrene (PHE), anthracene (ANT), fluoranthene (FLA), pyrene (PYR), benzo[a]anthracene (BaA), chrysene (CHR), benzo[b]fluoranthene (BbF), benzo[k]fluoranthene (BkF), benzo[a]pyrene (BaP), benzo[ghi]perylene (BghiP), dibenzo[a,h]anthracene (DbahA), and indeno[1,2,3-cd]pyrene (IP).

BEL2, BRA-C-05 and soil samples were analyzed on an HPLC-Fluo device (PerkinElmer 200 and 200a series) for 62 min according to the method described in Garagnon et al. (2023). MON-C-07 was analyzed on an UHPLC-Fluo (PerkinElmer, LC 300) with PAH elution performed on a C18 column equipped with a pre-column (EC 150/3 Nucleodur C18 PAH, Macherey-Nagel) maintained at 35 °C in an oven, for 20 min and according to the following program: 10 min at 1.2 mL min^{-1} with a 50:50 acetonitrile/water mixture, then increasing to 80:20 for 6 min and 100 % acetonitrile (Carlo Erba, for UHPLC-MS) for 3 min, ending with 1 min at 50:50 still at 1.2 mL min^{-1}. The quantification was calibrated by

an external method using 6 standard mixtures of 16 PAH reference materials (EPA 610).

Fluorescence detection was programmed with 9 pairs of excitation (225–333 nm) and emission (320–500 nm) wavelengths adapted to the sensitivity of each PAH (Garagnon et al., 2023). For each series, calibration was performed using 6 standards (from 1 to 80 ng mL^{-1}).

2.2.1.4. Quality control. The limits of detection (LOD) and quantification (LOQ) of the HPLC-Fluo were calculated using the calibration line method with three and six times the standard deviation of the y-intercepts and ranged from 0.02 to 0.21 ng g^{-1} for the LOD and 0.03–0.38 ng g^{-1} for the LOQ, depending on the PAHs considered. As these limits are higher than those of UHPLC (LOD <0.07 ng g^{-1} and LOQ <0.13 ng g^{-1}) they were applied to the sample measured with UHPLC for the sake of comparison. Procedural blanks following the same steps as the samples were analyzed. For USCDs, the limits of blanks (LOB) were lower than the concentrations measured in the samples, except for naphthalene and acenaphthene. For soils, the average blank values (between 0.01 and 5.35 ng g^{-1}) were all significantly lower than the concentrations measured in the samples. The deuterated PAHs were used as internal standards. The average yield of acenaphtene-d10, anthracene-d10, and benzo[a]anthracene-d-12 was 83 ± 30 %, 98 ± 20 % and 146 ± 25 % respectively for carbonates and 73 ± 19 %, 114 ± 25 % and 89 ± 20 % respectively for soils.

Values measured in samples below the LOD and LOB were considered to be zero. In addition, as the values in the USCDs were very low, it was decided to keep the values below the LOQ.

PAH uncertainties were calculated on the basis of deuterated PAH concentrations according to: $\frac{2\sigma}{\sqrt{n}} \times \frac{100}{\bar{x}}$ where, is the standard deviation, n, the number of measurements, and $\bar{x}$, the mean concentration. The calculation was applied on the basis of the physicochemical properties of each PAH (log K_{OC}; Table S3) according to three categories: PAHs with log $K_{OC} < 4$ (N, Ace, Flu), PAHs with log K_{OC} between 4 and 5 (Phe, Ant, Fla, Pyr), and PAHs with log $K_{OC} > 5$ (BaA, Chr, BbF, BkF, BaP, DbahA, BghiP, IP).

2.2.2. Carbon and organic matter analysis

2.2.2.1. USCD organic carbon. Glassware was washed in a hot detergent bath for 2 h, rinsed with osmosis water, dried, and calcined at 525 °C for 2 h to remove any organic residue.

For each USCD, approx. 80 mg of calcite powder were diluted with ultra-high quality (UHQ) water and then dissolved with HCl 12N (Carlo Elba, 34–37% RS Superpure for trace analysis) (Garagnon et al., 2023). Water and HCl volume were calculated for each sample to obtain 1 mL solution at neutral pH. After complete dissolution, the solution was diluted with UHQ water to a volume of 30 mL. After preparation, all samples were stored in a freezer and thawed 24 h prior to analysis.

Organic carbon (OC) analyses were performed on a Shimadzu TOC-V_{CSN} analyzer. Total carbon (TC) calibration between [0–20] mg.L^{-1} was performed using a Chemlab 100 ppm certified standard solution. Accuracy (99.5 %) and precision (relative standard deviation of 3%) were calculated by analyzing certified standard solutions (from Chemlab 100 ppm and Sigma standards 1000 mg.L^{-1}) and a home-made standard (from potassium hydrogen phthalate) at 5 mg.L^{-1} several times during the analytical sequence.

2.2.2.2. Soil organic carbon. Soil organic carbon (SOC) was estimated indirectly using the loss on ignition method. Approximately 10 mg of dry soil was calcined in ceramic pods at 550 °C for 4 h. The difference in mass before and after calcination is used to obtain the amount of soil organic matter (SOM). SOC is estimated using an empirical conversion factor such as: SOC = SOM/1.72 (Van Bemmelen, 1890; Waksman and Stevens, 1930).

2.2.2.3. Solid phase UV fluorescence (SPF). UV fluorescence analysis was performed on solid phase USCDs. An experimental spectrofluorometer was used. It is equipped with a thermoelectrically cooled, back-illuminated CCD detector (Jobin-Yvon Sincerity) and a monochromator (Jobin-Yvon MicroHr) with an adjustable slit and a 300 g/mm diffraction grating blazed at 450 nm and centered at 600 nm, giving a spectral resolution of about 1 nm/px (Garagnon et al., 2023). The organic material trapped in the USCD was then excited by two Nd:YAG lasers emitting at 266 nm and 355 nm. The 2-axis linear stage on which the sample was placed was used to measure steady-state laser-induced fluorescence (LIF) in two dimensions to obtain hyperspectral images with a resolution of 50 μm–100 μm.

2.2.3. Data processing

PAH and organic carbon data were analyzed and processed in Excel. The table of measured concentrations is provided in the supplementary material (Table S2). OC concentrations were corrected by the average UHQ water OC concentrations. The relative proportion of each PAH to the total of 15 PAHs was calculated to facilitate comparisons between sites as profiles. The percentage of PAHs with log $K_{OC} < 5$ (from N to Pyr), hereafter named weakly hydrophobic PAHs, was distinguished from those with log $K_{OC} > 5$ (from BaA to IP), hereafter named strongly hydrophobic PAHs, the latter having a very high affinity for OM.

Fluorescence spectra were simulated in Matlab using a supervised least-squares approach with a linear combination of log-normal functions constrained by ranges for position (in nm) and size (width and area) parameters (Moya et al., 2023). A mask was used to integrate only spectra within the area sampled for PAH analysis. Finally, 2 to 4 log-normal functions were used to simulate the fluorescence emission of organic matter, specifically including amino-acids (protein-like substances) (340 nm ± 20 nm) (Baker et al., 2008; Coble, 1996; Parlanti et al., 2000) and aromatic organic compounds formerly known as humic-like substances (420 nm ± 20 nm; 500 nm ± 20 nm) (Birdwell and Engel, 2010; Coble, 1996; Hudson et al., 2007).

2.3. Calculation

The concentration of PAHs in seepage water was not measured due to the large volumes of water required to exceed LOQ, so a theoretical calculation was used to attempt to predict the quantity of PAHs that could be dissolved in seepage water. The PAH concentrations in the seepage water were estimated using the following formula (Cousins et al., 1999): $\widehat{C}_w = \frac{C_{soil}}{K_{oc} \times f_{oc}}$ where C_{soil} is the PAH concentration in soil (ng.g_{soil}^{-1}); K_{oc} the partition constant between OM and water; and f_{oc} the fraction of organic carbon determined by the loss-on-ignition technique (g.g_{soil}^{-1}). The calculation was performed for an average value of K_{oc} for each PAH based on a literature review (Table S3). This calculation assumes that the water and solid phases are in equilibrium.

3. Results

3.1. PAHs in USCD

Sample BEL2, whose data have already been published in Garagnon et al. (2023), had the highest total PAH concentrations (sum of the 15 PAHs) (76.8 ± 5.3 ng g^{-1}), and a very high proportion of strongly hydrophobic PAHs (log $K_{OC} > 5$) (85.3 ± 5.4 %) especially BghiP (28.7 ± 1.8 %), IP (17.0 ± 1.1 %) and BaP (11.5 ± 0.7 %) (Fig. 2). Only 14.7 ± 1.4 % of weakly hydrophobic PAHs (log $K_{OC} < 5$) were present, mainly Pyr (6.6 ± 0.6 %), Fla (4.5 ± 0.4 %) and Phe (2.6 ± 0.3 %). In contrast, sample BRA-C-05 showed very low concentrations of total PAHs (Fig. 2), only 2.9 ± 0.4 ng g^{-1}, with a proportion of weakly hydrophobic PAHs of 100 ± 14.9 %, essentially dominated by Phe (40.5 ± 5.6 %) and Flu (34.0 ± 5.5 %). Sample MON-C-07 had a concentration of total PAHs of

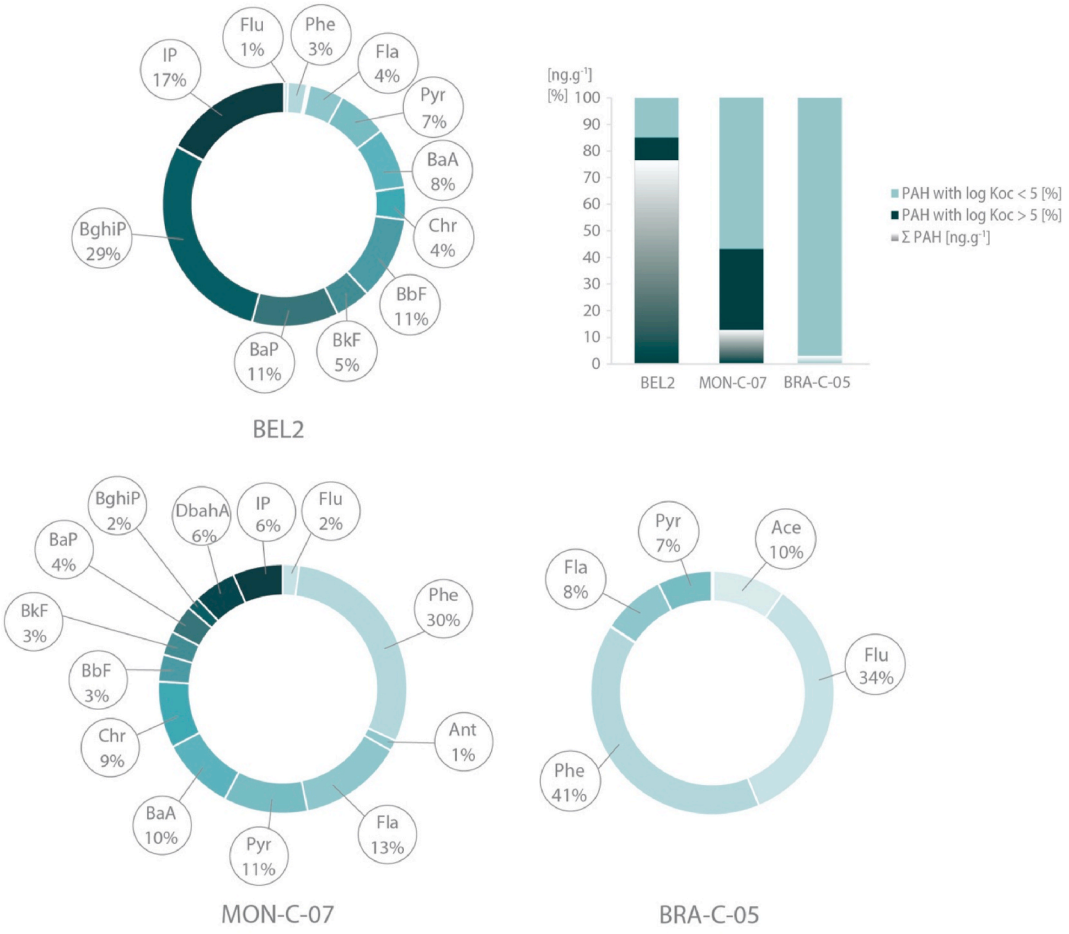

Fig. 2. PAH results in the different USCDs. The circles indicate the proportion (%) of each PAH relative to the total PAH concentration. The top-left histogram indicates both the proportion (%) of PAHs with log $K_{OC} < 5$, in light blue and PAHs with log $K_{OC} > 5$, in dark green, while the white limit corresponds to the total PAH concentration (ng.g^{-1}). (For interpretation of the references to color in this figure legend, the reader is referred to the Web version of this article.)

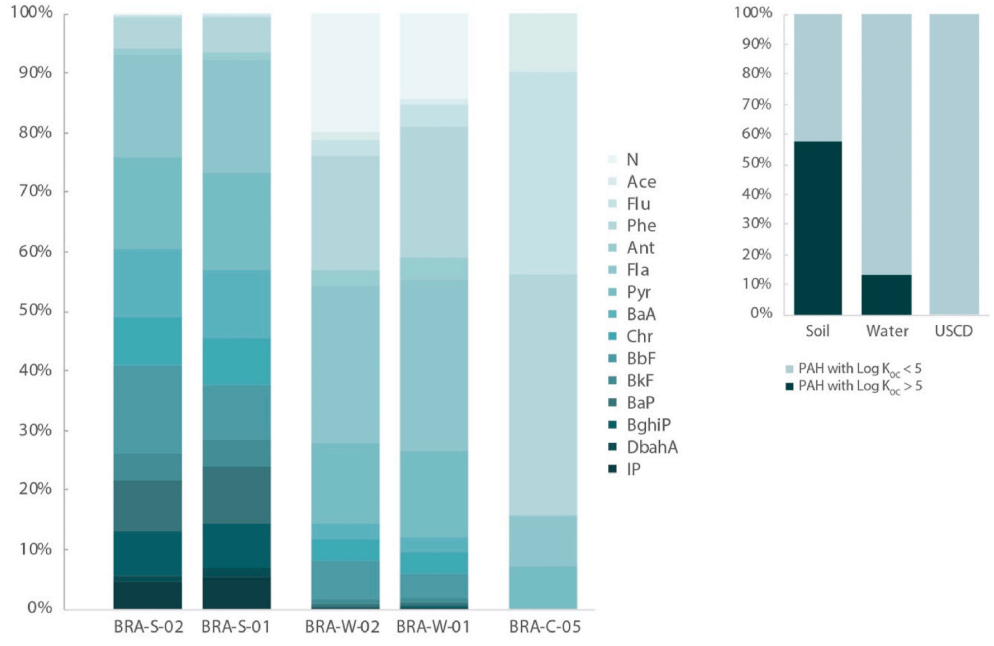

Fig. 3. PAH proportions relative to total PAHs (%) for the different materials at the Brasserie site. On the left, the detailed profile of the relative proportion of each PAH from least water soluble in dark to most water soluble in light with BRA-W-01 the theoretical prediction in seepage water from BRA-S-01 soil and BRA-W-02 the theoretical prediction in seepage water from BRA-S-02 soil. The graph on the right displays the average relative proportion of PAHs with log $K_{OC} < 5$ and PAHs with log $K_{OC} > 5$ for soils, for the theoretical prediction in seepage water and in USCD BRA-C-05.

12.8 ± 1.7 ng g^{-1} and a balanced distribution between strongly hydrophobic and weakly hydrophobic PAHs, respectively (42.3 ± 4.8 %) and (57.7 ± 8.1 %), essentially dominated by Phe (29.7 ± 4.1 %) and Fla (13.5 ± 1.9 %) (Fig. 2).

3.2. PAHs in soils

Compared to the USCDs, the soils had very high total PAH concentrations (Table S2): 2595 ± 355 ng g^{-1} for BRA-S-02 and 1914 ± 264 ng g^{-1} for BRA-S-01. The proportion of strongly hydrophobic PAHs (Fig. 3) was 60.3 ± 7.3 % for BRA-S-02 and 56.8 ± 7.1 % for BRA-S-01, while weakly hydrophobic PAHs accounted for 39.7 ± 6.2 % for BRA-S-02 and 43.2 ± 6.7 % for BRA-S-01. The profiles of the two samples are similar, with relatively high proportions of Fla, Pyr, BaA and BbF (Fig. 3): 18.1 ± 2.8 %, 16.0 ± 2.5 %, 11.3 ± 1.4 %, and 11.8 ± 1.5 %, respectively, on average.

3.3. Predicted PAH concentrations in seepage water

The distribution of weakly hydrophobic PAHs was obviously much greater than that of strongly hydrophobic PAHs, according to the theoretical prediction of PAHs dissolved in seepage water (BRA-W-01 and BRA-W-02) (Fig. 3). SOC quantity is underestimated of the black carbon content because of the loss of ignition procedure; the predicted PAH concentrations in seepage water are therefore overestimated. For the sample BRA-S-02 (i.e. BRA-W-02), 85.7 % of the PAHs had log K_{OC} < 5, while only 14.3 % had log K_{OC} > 5. For the BRA-W-01, the percentages were 88.0 % and 12.0 %, respectively. The dominant PAHs in the seepage water were Phe and Fla, averaging 20.4 % and 27.4 % (Fig. 3). Total PAH concentrations ranged from 2019 ng.L^{-1} for BRA-W-02 and 1482 ng.L^{-1} for BRA-W-01, as shown in Table S2.

3.4. Organic carbon

In soil samples, the concentration of organic carbon (OC) appeared to decrease with depth. For instance, BRA-S-02 had an OC concentration of 55.3 mg. g_{soil}^{-1} at a depth of 0–10 cm, while BRA-S-01 had an OC concentration of 18.1 mg. g_{soil}^{-1} at a depth of 20–30 cm (Fig. 4). The highest OC concentration in the USCD was found in sample BEL2 (2.7 ± 0.2 mg g_{CaCO3}^{-1}), while the lowest was found in BRA-C-05 (0.7 ± 0.1 mg. g_{CaCO3}^{-1}). MON-C-07 contained 0.9 ± 0.1 mg. g_{CaCO3}^{-1} (Fig. 4).

3.5. Organic matter content

Fluorescence simulation of the average spectrum at the top of each USCD highlighted the different types of chromophoric OM present in each (Fig. 5). Under 266 nm excitation, the BRA-C-05 spectrum exhibited a shoulder around 350 nm corresponding to aromatic amino acid-type organic molecules. These molecules appeared to be less present in BEL2 and MON-C-07. However, these compounds were in a low proportion (≤1 %) compared to aromatic organic compounds. Two aromatic organic groups were identified, the first (with excitation/emission wavelengths (λex./λem.) of 266/430–440 nm and 355/420 nm) corresponding to aromatic substances with some aliphatic chains, and the second with larger aromatic compounds emitting around 475–500 nm. The first group was clearly dominant for MON-C-07 (59 %) and BRA-C-05 (70 %). BRA-C-05 also contained molecules emitting at higher wavelengths (λem. ≈ 560 nm) when excited at 266 nm, which could correspond to heavier molecular weight organic matter or manganese-substituted calcium (El Ali et al., 1993; Machel et al., 1991). Excitation at 355 nm also revealed a molecular group emitting around 530 nm, which may be associated with highly aromatic organic compounds.

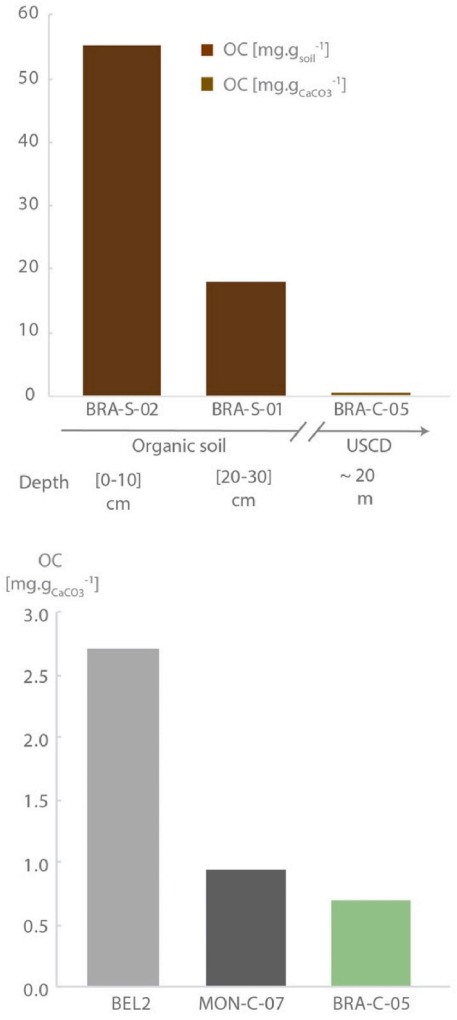

Fig. 4. The histograms represent organic carbon concentrations: at the top, in soils (mg.g_{soil}^{-1}) and in USCD BRA-S-05 (mg.g_{CaCO3}^{-1}) at the Brasserie site; at the bottom, in the three USCDs (mg.g_{CaCO3}^{-1}).

4. Discussion

4.1. PAH retention by organic soil

The Brasserie site is the only site investigated where organic soil is present. The soil samples revealed very high concentrations of total PAHs with 2595 ng. g_{soil}^{-1} in the surface horizon and 1914 ng. g_{soil}^{-1} in the deeper horizon (Fig. 6), comparable to the range of concentrations measured in other parks and gardens in Paris (512–8767 ng g^{-1}) (unpublished data from Cerema) and to data reported in studies of urban soils in Europe, e. g, 2538 ng g^{-1} on average in Bratislava (Bandowe et al., 2011), 1544 ng g^{-1} in Lisbon (Cachada et al., 2012), or 1990 ng g^{-1} in Turin (Morillo et al., 2007). In addition, soil OC concentrations in the surface horizon (55.25 mg. g_{soil}^{-1}) were 3 times higher than in the deep horizon (18.12 mg. g_{soil}^{-1}).

The average PAH profile obtained in the Brasserie soils is also very close to that of the average annual atmospheric deposition in Paris (data from Ollivon et al., 2002, Fig. 6), with the same PAHs present and a correlation of 0.80 between the two profiles. Although a partitioning between atmospheric deposits and soils is observed: proportionally, the strongly hydrophobic PAHs, which tend to adsorb strongly onto OM, are dominant in the soils. The low molecular weight PAHs (such as naphthalene) are volatilized to the atmosphere (Park et al., 1990), biodegraded by soil microbial communities, or transferred by seepage

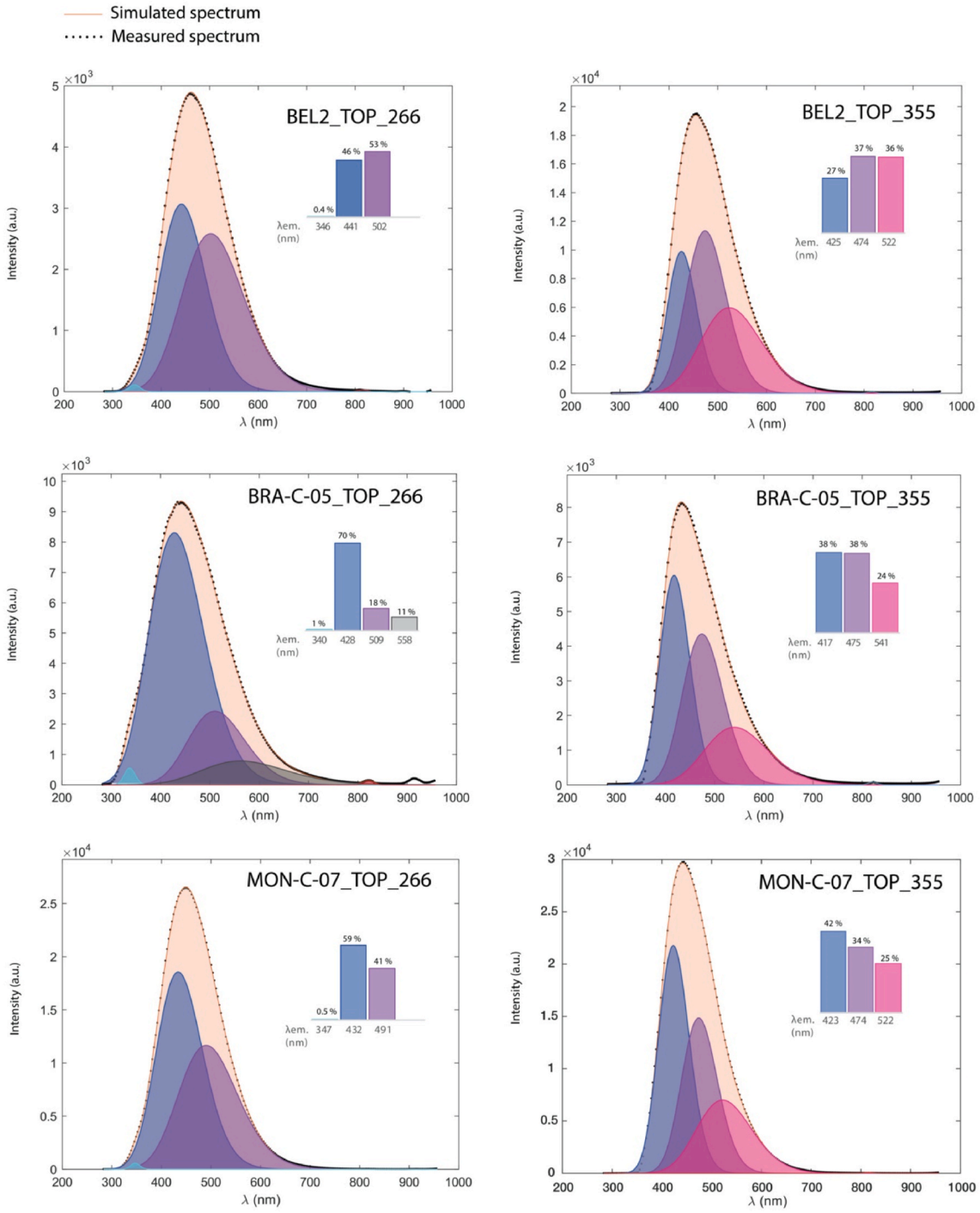

Fig. 5. Result of the average spectral simulation for each sample at 266 nm and 355 nm excitation and the proportion (%) of each fluorophore present. The light blue emission centered at around 350 nm visible under 266 nm excitation corresponds to amino acids, the dark blue, violet and pink emissions correspond to aromatic organic compounds and the black area is probably associated to Mn^{2+}. (For interpretation of the references to color in this figure legend, the reader is referred to the Web version of this article.)

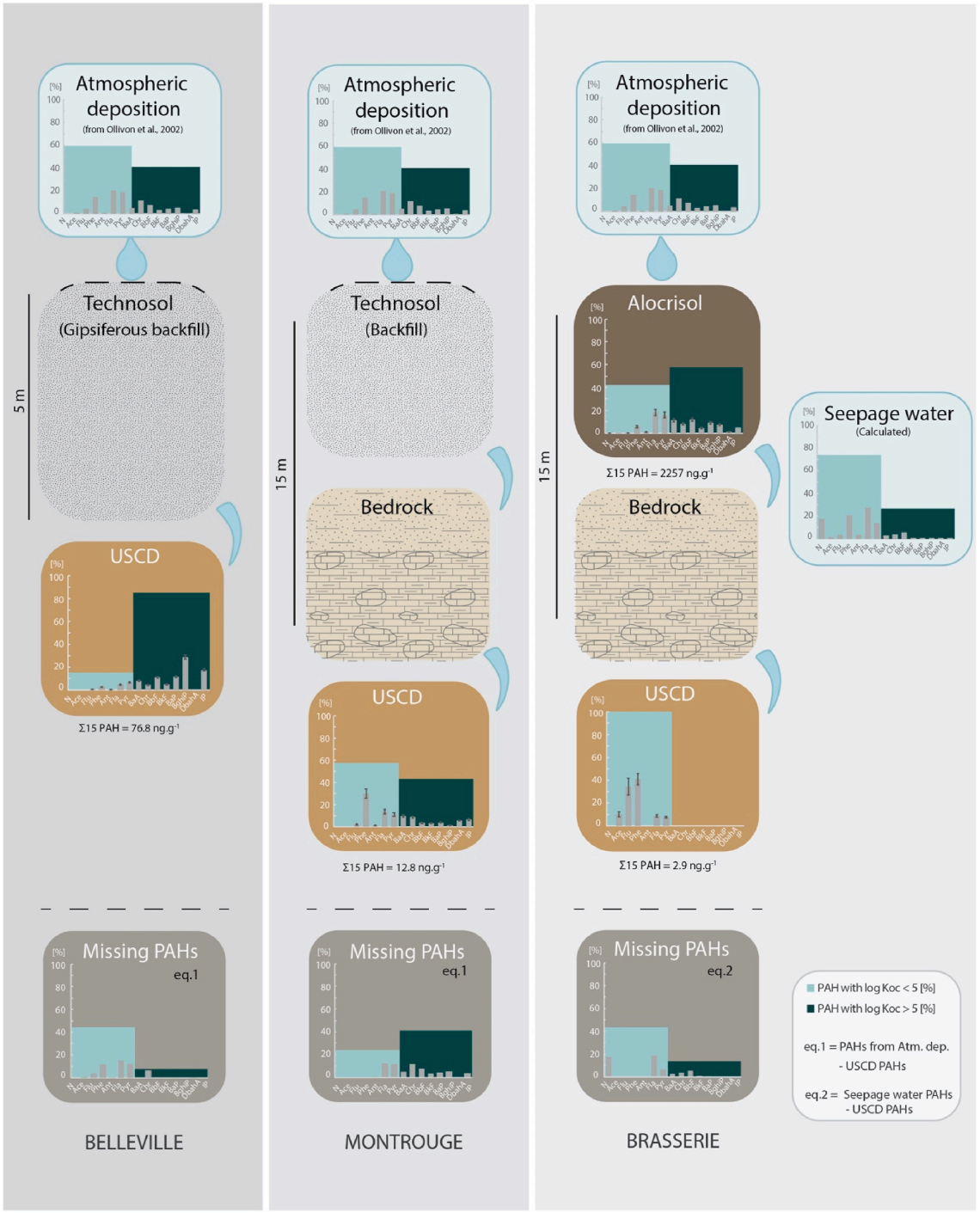

Fig. 6. Schematic summary of PAH concentrations in each compartment (measurements in soil and USCD and theoretical calculations in seepage water) for each of the three sites. Missing PAHs correspond to the proportion of PAHs lost during transport (eq. 1 and 2). The source considered for Belleville and Montrouge corresponds to the average dry and wet atmospheric deposition in Paris (Ollivon et al., 2002).

water in dissolved or particulate form (Wild and Jones, 1995). Theoretical calculations of PAH concentrations in dissolved form in the seepage water (Figs. 3 and 6) show a clear predominance of weakly hydrophobic PAHs (86–88 %). In addition, USCD BRA-C-05, located about 15 m below the investigated soil, contains a low amount of total PAH (2.9 ng. g^{-1}_{CaCO3}) and contain exclusively weakly hydrophobic PAHs. All these elements point to a retention of the strongly hydrophobic PAHs (BkF to IP) in the soils, due to a high sorption onto SOM (Jones et al., 1989; Santschi et al., 1997). The presence of organic soil therefore appears to play a key role in the retention of PAHs. Numerous studies have already demonstrated the ability of SOM to retain contaminants in soils, thereby improving and protecting water quality (e.g. Lehmann and Kleber, 2015).

However, the theoretical PAH profile of the infiltration water is not identical to that of BRA-C-05. The difference between the two ("Missing PAHs" in Fig. 6) could be explained by: (i) a retention effect by the bedrock, in particular the strongly hydrophobic PAHs, (ii) an unknown partitioning effect between water and calcite or, (iii) as in soils, a biodegradation process by microbial communities present in the water, forming methylated or hydroxylated metabolites. As PAHs with less than 3–4 aromatic rings are the most soluble and biodegradable (Gupta et al., 2015), these last two hypotheses would especially explain the difference in signatures of weakly hydrophobic PAHs.

4.2. Influence of depth and lithology on PAH transferred to the USCD

Sample BEL2 contains 76.8 ng g^{-1} of total PAH (Table S2). In contrast, concentrations in the other two USCDs, MON-C-07 and BRA-C-05, are 6–26 times lower (12.8 and 2.9 ng g^{-1} respectively). Moreover, BEL2 also contains the highest OC concentration (2.7 mg g^{-1}_{CaCO3}) and a higher proportion (53 %) of highly aromatic organic compounds than BRA-C-05 and MON-C-07 (Fig. 5).

However, BEL2 is located at a shallower depth and is topped by a backfill whereas MON-C-07 and BRA-C-05 were both sampled at a depth of more than 15 m and are topped by a layer of sand and a layer of limestone rich in marl (Fig. 1). In addition, the three sites are less than 10 km apart and are located at a comparable distance (≈1 km) from the main Paris ring road, thus it is assumed that atmospheric depositions between the three sites are similar. Considering the annual dry and wet atmospheric deposition measured in Paris by Ollivon et al. (2002) as the main common source of PAHs for all sites, the thickness and quality of the rock column infiltrated by the seepage water probably play a major role in PAH retention.

The proximity of BEL2 to the urbanized soil surface could be responsible for its high PAH and OC concentrations. Most strongly hydrophobic PAHs have migrated to the USCD as revealed by the PAH profiles of the atmospheric deposits in Paris and of the BEL2 sample (Fig. 6). Some weakly hydrophobic PAHs are not present in the USCD: they could have been biodegraded or, if not, they could be kept in aqueous phase (i.e. not trapped in the USCD) because of their low K_{OC}. Besides, the portion of the aqueduct where BEL2 was sampled is located almost below Levert street. Thus, in addition to atmospheric deposition, seepage water can also drain urban dust via road runoff containing more heavy molecular weight PAHs deposited on the surface (Garagnon et al., 2023; Gasperi et al., 2014). However, comparison with other PAH sources (Urban dust, Road runoff) (Fig. S4) shows comparable results. The relatively low permeability of the Beauchamp sands at the Montrouge and Brasserie sites (hydraulic conductivity (K) ranges from 1.10^{-5} and 1.10^{-4} m s^{-1}, Laboratoire Régional des Ponts et Chaussées de l'Est Parisiens, 2002), reinforced by the underlying marly limestones of the Upper Lutecian, can efficiently retain the aromatic moieties of OM and the more strongly hydrophobic PAHs. Indeed, the transfer of low-molecular-weight (or less aromatic) OMs seems to be favored at these sites (Fig. 5). In addition, most of the PAHs less present in MON-C-07 compared to the atmospheric deposits ("Missing PAH" in Fig. 6) are strongly hydrophobic PAHs, generally in particulate form in the natural waters (Cao et al., 2024; Guo et al., 2007). As a comparison, column filtration experiments of urban runoff water have demonstrated their potential to remove over 90% of PAHs through different media such as sand or calcite (Prabhukumar et al., 2015; Reddy et al., 2014).

Although located at equivalent depths, the total PAH concentration in MON-C-07 is significantly higher than in BRA-C-05. Even if the influence of a possible difference in facies (more or less rich in sands or marl and of different thickness) between the two sites cannot be excluded, this fourfold decrease in PAH concentration in BRA-C-05 can be more easily explained by the presence of the organic soil at the Brasserie site. In the absence of organic soil at the Montrouge site, some strongly hydrophobic PAHs are present in MON-C-07. Besides, BEL2 and MON-C-07 contain both a significant proportion (respectively 85 % and 42 %) of strongly hydrophobic, bioaccumulable and often carcinogenic and mutagenic PAHs (IARC, 2023; US EPA, 1985). These PAHs are absent in BRA-C-05 (Figs. 2 and 6) because of their probable sorption onto the organic soil, which seems essential for the preservation of groundwater quality.

This study assumed that the three USCDs are fed by seepage water from the soil directly above the aqueduct and quarry. Yet detailed hydrogeological studies would be appreciated, as surface soil sealing raises questions about the origin of the water and how it infiltrates (e.g. green spaces, private gardens, leaks from stormwater networks).

5. Conclusion

During the infiltration of surface water through the soil and bedrock, dissolved and particulate PAHs undergo complex interactions with the solid phase, depending on their K_{OC}, as revealed by the comparison of their profile distribution in the assumed main source (atmospheric deposition) and in different USCDs sampled in Paris. The bedrock lithology and thickness (between surface and USCD) play an important role in the retention of PAHs, especially those adsorbed on the particulate phase. However, organic soils, as a natural OC-rich reservoir, can store high amounts of PAHs, especially the more strongly hydrophobic ones, which are also the more lipophilic therefore bioaccumulable and toxic. Hence, USCDs have demonstrated their potential as water quality archives of the water composition. However, further research is needed to study the process of PAH trapping in calcite and identify possible fractionation. Extending this work to other contaminant families and other study sites, coupled with detailed hydrogeological studies, could improve our knowledge of near-surface water quality and contaminant transfer in urban environments. Indeed, land-use change is the first stage in the development of an urban area. In a world where water access will become increasingly complex, it seems extremely important to preserve groundwater quality by avoiding soil sealing and maintaining the OC richness of surface soils.

CRediT authorship contribution statement

Julia Garagnon: Writing – review & editing, Writing – original draft, Visualization, Validation, Methodology, Investigation, Formal analysis. **Emmanuel Naffrechoux:** Writing – review & editing, Validation, Supervision, Conceptualization. **Yves Perrette:** Writing – review & editing, Supervision, Software, Conceptualization. **Emmanuel Dumont:** Writing – review & editing, Investigation. **Phillipe Branchu:** Writing – review & editing, Investigation. **Jules Querleux:** Writing – review & editing, Investigation. **Gael Monvoisin:** Writing – review & editing, Investigation. **Mathieu Pin:** Writing – review & editing, Formal analysis. **Delphine Tisserand:** Writing – review & editing, Formal analysis. **Edwige Pons-Branchu:** Writing – review & editing, Supervision, Resources, Project administration, Funding acquisition, Conceptualization.

Declaration of competing interest

The authors declare that they have no known competing financial interests or personal relationships that could have appeared to influence the work reported in this paper.

Data availability

Data will be made available on request.

Acknowledgements

The ASNEP - Association Sources du Nord - Études et Préservation, the Mairie de Paris (Département des Édifices Cultuels et Historiques — Direction des Affaires Culturelles) and the Inspection Générale des Carrières are thanked for giving access to the Belleville aqueduct and historical information. TC analyses were performed using the geochemistry-mineralogy platform of ISTerre (OSUG-France). N. Cottin and V. Naffrechoux (EDYTEM/USMB) are also thanked for their advice on the analytical procedures. This work was supported by the "HUNIWERS" project from the ANR (grant number 18- CE22-0009) and by the "Recherche Elan 2023" project from the Graduate School Geosciences, Climate, Environment, Planets of the University of Paris-Saclay.

Appendix A. Supplementary data

Supplementary data to this article can be found online at https://doi.org/10.1016/j.envpol.2024.124437.

References

AFES, 2008. Référentiel Pédologique 2008. Editions Quae, Paris, France.
Arias, A.H., Vazquez-Botello, A., Tombesi, N., Ponce-Vélez, G., Freije, H., Marcovecchio, J., 2010. Presence, distribution, and origins of polycyclic aromatic hydrocarbons (PAHs) in sediments from Bahía Blanca estuary, Argentina. Environ. Monit. Assess. 160, 301–314. https://doi.org/10.1007/s10661-008-0696-5.
Ayrault, S., Meybeck, M., Mouchel, J.-M., Gaspéri, J., Lestel, L., Lorgeoux, C., Boust, D., 2021. Sedimentary archives reveal the Concealed history of Micropollutant contamination in the seine river basin. In: Flipo, N., Labadie, P., Lestel, L. (Eds.), The Seine River Basin, the Handbook of Environmental Chemistry. Springer International Publishing, Cham, pp. 269–300. https://doi.org/10.1007/698_2019_386.
Baker, A., Tipping, E., Thacker, S.A., Gondar, D., 2008. Relating dissolved organic matter fluorescence and functional properties. Chemosphere 73, 1765–1772. https://doi.org/10.1016/j.chemosphere.2008.09.018.
Bandowe, B.A.M., Sobocka, J., Wilcke, W., 2011. Oxygen-containing polycyclic aromatic hydrocarbons (OPAHs) in urban soils of Bratislava, Slovakia: Patterns, relation to PAHs and vertical distribution. Environ. Pollut. 159, 539–549. https://doi.org/10.1016/j.envpol.2010.10.011.
Birdwell, J.E., Engel, A.S., 2010. Characterization of dissolved organic matter in cave and spring waters using UV–Vis absorbance and fluorescence spectroscopy. Org. Geochem. 41, 270–280. https://doi.org/10.1016/j.orggeochem.2009.11.002.
Brown, J.N., Peake, B.M., 2006. Sources of heavy metals and polycyclic aromatic hydrocarbons in urban stormwater runoff. Sci. Total Environ. 359, 145-155.
Brown, J.R., Field, R.A., Goldstone, M.E., Lester, J.N., Perry, R., 1996. Polycyclic aromatic hydrocarbons in central London air during 1991 and 1992. Sci. Total Environ. 177, 73–84. https://doi.org/10.1016/0048-9697(95)04866-9.
Burri, N.M., Weatherl, R., Moeck, C., Schirmer, M., 2019. A review of threats to groundwater quality in the anthropocene. Sci. Total Environ. 684, 136–154. https://doi.org/10.1016/j.scitotenv.2019.05.236.
Cachada, A., Pato, P., Rocha-Santos, T., da Silva, E.F., Duarte, A.C., 2012. Levels, sources and potential human health risks of organic pollutants in urban soils. Sci. Total Environ. 430, 184–192. https://doi.org/10.1016/j.scitotenv.2012.04.075.
Cao, Y., Wang, J., Xin, M., Wang, B., Lin, C., 2024. Spatial distribution and partition of polycyclic aromatic hydrocarbons (PAHs) in the water and sediment of the southern Bohai Sea: Yellow River and PAH property influences. Water Res. 248, 120873 https://doi.org/10.1016/j.watres.2023.120873.
Clément, A., Thomas, G., 2016. In: Atlas du Paris souterrain: la doublure sombre de la Ville lumière. Parigramme, Paris.
Coble, P.G., 1996. Characterization of marine and terrestrial DOM in seawater using excitation-emission matrix spectroscopy. Mar. Chem. 51, 325–346. https://doi.org/10.1016/0304-4203(95)00062-3.
Coleman, P.J., Lee, R.G.M., Alcock, R.E., Jones, K.C., 1997. Observations on PAH, PCB, and PCDD/F Trends in U.K. Urban air, 1991−1995. Environ. Sci. Technol. 31, 2120–2124. https://doi.org/10.1021/es960953q.
Cousins, I.T., Beck, A.J., Jones, K.C., 1999. A review of the processes involved in the exchange of semi-volatile organic compounds (SVOC) across the air–soil interface. Sci. Total Environ. 228, 5–24. https://doi.org/10.1016/S0048-9697(99)00015-7.
Du, J., Jing, C., 2018. Anthropogenic PAHs in lake sediments: a literature review (2002–2018). Environ. Sci.: Process. Impacts 20, 1649–1666. https://doi.org/10.1039/C8EM00195B.
El Ali, A., Barbin, V., Calas, G., Cervelle, B., Ramseyer, K., Bouroulec, J., 1993. Mn2+-activated luminescence in dolomite, calcite and magnesite: quantitative determination of manganese and site distribution by EPR and CL spectroscopy. Chem. Geol. 104, 189–202. https://doi.org/10.1016/0009-2541(93)90150-H.
FAO, 2006. World reference base for soil resources 2006: a framework for international classification, correlation, and communication. In: World soil resources reports, 103. FAO, Rome, Italy.
Flörke, M., Schneider, C., McDonald, R.I., 2018. Water competition between cities and agriculture driven by climate change and urban growth. Nat. Sustain. 1, 51–58. https://doi.org/10.1038/s41893-017-0006-8.
Garagnon, J., Perrette, Y., Naffrechoux, E., Pons-Branchu, E., 2023. Polycyclic aromatic hydrocarbon record in an urban secondary carbonate deposit over the last three centuries (Paris, France). Sci. Total Environ. 905, 167429 https://doi.org/10.1016/j.scitotenv.2023.167429.
Gasperi, J., Sebastian, C., Ruban, V., Delamain, M., Percot, S., Wiest, L., Mirande, C., Caupos, E., Demare, D., Kessoo, M.D.K., Saad, M., Schwartz, J.J., Dubois, P., Fratta, C., Wolff, H., Moilleron, R., Chebbo, G., Cren, C., Millet, M., Barraud, S., Gromaire, M.C., 2014. Micropollutants in urban stormwater: occurrence, concentrations, and atmospheric contributions for a wide range of contaminants in three French catchments. Environ. Sci. Pollut. Res. 21, 5267–5281. https://doi.org/10.1007/s11356-013-2396-0.
Genty, D., Quinif, Y., 1996. Annually laminated sequences in the internal structure of some Belgian stalagmites; importance for paleoclimatology. J. Sediment. Res. 66, 275–288. https://doi.org/10.1306/D426831A-2B26-11D7-8648000102C1865D.
Guo, W., He, M., Yang, Z., Lin, C., Quan, X., Wang, H., 2007a. Distribution of polycyclic aromatic hydrocarbons in water, suspended particulate matter and sediment from Daliao River watershed, China. Chemosphere 68, 93–104. https://doi.org/10.1016/j.chemosphere.2006.12.072.
Guo, Z., Lin, T., Zhang, G., Zheng, M., Zhang, Z., Hao, Y., Fang, M., 2007b. The sedimentary fluxes of polycyclic aromatic hydrocarbons in the Yangtze River Estuary coastal sea for the past century. Sci. Total Environ. 386, 33–41. https://doi.org/10.1016/j.scitotenv.2007.07.019.
Gupta, S., Pathak, B., Fulekar, M.H., 2015. Molecular approaches for biodegradation of polycyclic aromatic hydrocarbon compounds: a review. Rev. Environ. Sci. Biotechnol. 14, 241–269. https://doi.org/10.1007/s11157-014-9353-3.
Hudson, N., Baker, A., Reynolds, D., 2007. Fluorescence analysis of dissolved organic matter in natural, waste and polluted waters—a review. River Res. Appl. 23, 631–649. https://doi.org/10.1002/rra.1005.
Inspection Générale des Carrières, 2007. Atlas des carrières souterraines de Paris. https://www.arcgis.com/apps/instant/media/index.html?appid=59873b0b206e4aefae712dc2cdda200c.
International Agency for Research on Cancer, 2023. Monographs on the Identification of Carcinogenic Hazards to Humans 1–134. https://monographs.iarc.who.int/list-of-classifications/. accessed 2.6.24.
IUSS Working Group WRB, 2022. World reference base for soil resources. In: International Soil Classification System for Naming Soils and Creating Legends for Soil Maps, fourth ed. International Union of Soil Sciences (IUSS), Vienna Austria.
Jones, K.C., Stratford, J.A., Tidridge, P., Waterhouse, K.S., Johnston, A.E., 1989. Polynuclear aromatic hydrocarbons in an agricultural soil: long-term changes in profile distribution. Environ. Pollut. 56, 337–351. https://doi.org/10.1016/0269-7491(89)90079-1.
Laboratoire Régional des Ponts et Chaussées de l'Est Parisiens, 2002. CDG Express - Projet de liaison ferroviaire rapide entre la Gare de l'Est et l'Aéroport Charles de Gaulle - Etude hydrogéologique documentaire de la partie souterraine du projet. Le Bourget, France.
Lan, J., Sun, Y., Yuan, D., 2018. Transport of polycyclic aromatic hydrocarbons in a highly vulnerable karst underground river system of southwest China. Environ. Sci. Pollut. Res. 25, 34519–34530. https://doi.org/10.1007/s11356-018-3005-z.
Lehmann, J., Kleber, M., 2015. The contentious nature of soil organic matter. Nature 528, 60–68. https://doi.org/10.1038/nature16069.
Ligtvoet, W., Hilderink, H., Bouwman, A., Puijenbroek, P., Lucas, P., Witmer, M., 2014. Towards a World of Cities in 2050 - an Outlook on Water- Related Challenges (Background Report to the UN-habitat Global Report). PBL Netherlands Environmental Assessment Agency.
Machel, H.G., Mason, R.A., Mariano, A.N., Mucci, A., 1991. Causes and emission of luminescence in calcite and dolomite. In: Barker, C.E., Burruss, R.C., Kopp, O.C., Machel, H.G., Marshall, D.J., Wright, P., Colbum, H.Y. (Eds.), Luminescence Microscopy and Spectroscopy: Qualitative and Quantitative Applications. SEPM Society for Sedimentary Geology. https://doi.org/10.2110/scn.91.25.0009, 0.
Marchal, L., Gateuille, D., Naffrechoux, E., Deline, P., Baudin, F., Clement, J.-C., Poulenard, J., 2023. Polycyclic aromatic hydrocarbon dynamics in soils along proglacial chronosequences in the Alps. Sci. Total Environ. 902, 165998 https://doi.org/10.1016/j.scitotenv.2023.165998.
Morillo, E., Romero, A.S., Maqueda, C., Madrid, L., Ajmone-Marsan, F., Grcman, H., Davidson, C.M., Hursthouse, A.S., Villaverde, J., 2007. Soil pollution by PAHs in urban soils: a comparison of three European cities. J. Environ. Monit. 9, 1001–1008. https://doi.org/10.1039/B705955H.
Moya, A., Giraud, F., Molinier, V., Perrette, Y., Charlet, L., Van Driessche, A., Fernandez-Martinez, A., 2023. Exploring carbonate rock wettability across scales: role of (bio)

minerals. J. Colloid Interface Sci. 642, 747–756. https://doi.org/10.1016/j.jcis.2023.03.197.
Müller, A., Österlund, H., Marsalek, J., Viklander, M., 2020. The pollution conveyed by urban runoff: a review of sources. Sci. Total Environ. 709, 136125 https://doi.org/10.1016/j.scitotenv.2019.136125.
Nielsen, T., Jørgensen, H.E., Larsen, J.Chr, Poulsen, M., 1996. City air pollution of polycyclic aromatic hydrocarbons and other mutagens: occurrence, sources and health effects. Sci. Total Environ. 189–190, 41–49. https://doi.org/10.1016/0048-9697(96)05189-3.
Ollivon, D., Blanchoud, H., Motelay-Massei, A., Garban, B., 2002. Atmospheric deposition of PAHs to an urban site, Paris, France. Atmos. Environ. 36, 2891–2900. https://doi.org/10.1016/S1352-2310(02)00089-4.
Park, K.S., Sims, R.C., Dupont, R.R., Doucette, W.J., Matthews, J.E., 1990. Fate of PAH compounds in two soil types: influence of volatilization, abiotic loss and biological activity. Environ. Toxicol. Chem. 9, 187–195. https://doi.org/10.1002/etc.5620090208.
Parlanti, E., Wörz, K., Geoffroy, L., Lamotte, M., 2000. Dissolved organic matter fluorescence spectroscopy as a tool to estimate biological activity in a coastal zone submitted to anthropogenic inputs. Org. Geochem. 31, 1765–1781. https://doi.org/10.1016/S0146-6380(00)00124-8.
Pereira, W.E., Hostettler, F.D., Luoma, S.N., Van Geen, A., Fuller, C.C., Anima, R.J., 1999. Sedimentary record of anthropogenic and biogenic polycyclic aromatic hydrocarbons in San Francisco Bay, California. Mar. Chem. 64, 99–113. https://doi.org/10.1016/S0304-4203(98)00087-5.
Perrette, Y., Poulenard, J., Saber, A.-I., Fanget, B., Guittonneau, S., Ghaleb, B., Garaudee, S., 2008. Polycyclic Aromatic Hydrocarbons in stalagmites: occurrence and use for analyzing past environments. Chem. Geol. 251, 67–76. https://doi.org/10.1016/j.chemgeo.2008.02.013.
Pons-Branchu, E., Ayrault, S., Roy-Barman, M., Bordier, L., Borst, W., Branchu, P., Douville, E., Dumont, E., 2015. Three centuries of heavy metal pollution in Paris (France) recorded by urban speleothems. Sci. Total Environ. 518–519, 86–96. https://doi.org/10.1016/j.scitotenv.2015.02.071.
Pons-Branchu, E., Douville, E., Roy-Barman, M., Dumont, E., Branchu, P., Thil, F., Frank, N., Bordier, L., Borst, W., 2014. A geochemical perspective on Parisian urban history based on U–Th dating, laminae counting and yttrium and REE concentrations of recent carbonates in underground aqueducts. Quat. Geochronol. 24, 44–53. https://doi.org/10.1016/j.quageo.2014.08.001.
Pons-Branchu, E., Roy-Barman, M., Jean-Soro, L., Guillerme, A., Branchu, P., Fernandez, M., Dumont, E., Douville, E., Michelot, J., Phillips, A., 2017. Urbanization impact on sulfur content of groundwater revealed by the study of urban speleothem-like deposits: Case study in Paris, France. Sci. Total Environ. 579, 124–132. https://doi.org/10.1016/j.scitotenv.2016.10.234.
Prabhukumar, G., Bhupal, G.S., Pagilla, K.R., 2015. Laboratory Evaluation of sorptive filtration media mixtures for Targeted pollutant Removals from simulated stormwater. Water Environ. Res. 87, 789–795. https://doi.org/10.2175/106143015X14362865226239.
Reddy, K.R., Xie, T., Dastgheibi, S., 2014. PAHs removal from urban Storm water runoff by different filter materials. Journal of Hazardous, Toxic, and Radioactive Waste 18, 04014008. https://doi.org/10.1061/(ASCE)HZ.2153-5515.0000222.
Santschi, P.H., Lenhart, J.J., Honeyman, B.D., 1997. Heterogeneous processes affecting trace contaminant distribution in estuaries: the role of natural organic matter. Mar. Chem. 58, 99–125. https://doi.org/10.1016/S0304-4203(97)00029-7.
Schwarz, K., Gocht, T., Grathwohl, P., 2011. Transport of polycyclic aromatic hydrocarbons in highly vulnerable karst systems. Environ. Pollut. 159, 133–139. https://doi.org/10.1016/j.envpol.2010.09.026.
Simcik, M.F., Zhang, H., Eisenreich, S.J., Franz, T.P., 1997. Urban contamination of the Chicago/coastal lake Michigan atmosphere by PCBs and PAHs during AEOLOS. Environ. Sci. Technol. 31, 2141–2147. https://doi.org/10.1021/es9609765.
Takada, H., Onda, T., Harada, M., Ogura, N., 1991. Distribution and sources of polycyclic aromatic hydrocarbons (PAHs) in street dust from the Tokyo Metropolitan area. Sci. Total Environ. 107, 45–69. https://doi.org/10.1016/0048-9697(91)90249-E.
United Nations, Population Division, 2019. World Urbanization Prospects: the 2018 Revision. United Nations, Department of Economic and Social Affairs, New York.
US EPA, 1985. Evaluation and estimation of potential carcinogenic risks of polynuclear aromatic hydrocarbons (PAH). Office of Health and Environmental Assessment. US EPA, Washington, DC.
Van Bemmelen, J.M., 1890. Über die Bestimmung des Wassers, des Humus, des Schwefels, der in den colloïdalen Silikaten gebundenen Kieselsäure. des Mangans u. s. w. im Ackerboden. Die Landwirthschaftlichen Versuchs-Stationen 37, 279–290.
Waksman, S.A., Stevens, K.R., 1930. A critical study of the methods for determining the nature and abundance of soil organic matter. Soil Sci. 30, 97–116. https://doi.org/10.1097/00010694-193008000-00002.
Wild, S.R., Jones, K.C., 1995. Polynuclear aromatic hydrocarbons in the United Kingdom environment: a preliminary source inventory and budget. Environ. Pollut. 88, 91–108. https://doi.org/10.1016/0269-7491(95)91052-M.